nature nanotechnology

LETTERS

PUBLISHED ONLINE: 19 FEBRUARY 2012 | DOI: 10.1038/NNANO.2012.19

Engineering controllable bidirectional molecular motors based on myosin

Lu Chen[1], Muneaki Nakamura[1,2], Tony D. Schindler[1], David Parker[1] and Zev Bryant[1,3]*

Cytoskeletal motors drive the transport of organelles and molecular cargoes within cells[1] and have potential applications in molecular detection and diagnostic devices[2,3]. Engineering molecular motors with controllable properties will allow selective perturbation of mechanical processes in living cells and provide optimized device components for tasks such as molecular sorting and directed assembly[3]. Biological motors have previously been modified by introducing activation/deactivation switches that respond to metal ions[4,5] and other signals[6]. Here, we show that myosin motors can be engineered to reversibly change their direction of motion in response to a calcium signal. Building on previous protein engineering studies[7–11] and guided by a structural model[12] for the redirected power stroke of myosin VI, we have constructed bidirectional myosins through the rigid recombination of structural modules. The performance of the motors was confirmed using gliding filament assays and single fluorophore tracking. Our strategy, in which external signals trigger changes in the geometry and mechanics of myosin lever arms, should make it possible to achieve spatiotemporal control over a range of motor properties including processivity, stride size[13] and branchpoint turning[14].

Controllable bidirectional motion is a basic feature of many man-made machines and is critical to the function of biological systems such as the bacterial flagellar motor, which reverses its direction of rotation in response to cellular signaling[15]. Bidirectional transport on cytoskeletal filaments is generally thought to rely on the alternate engagement of distinct motors with differing fixed polarities, although context-dependent directionality has recently been observed in a mitotic kinesin[16]. No motors have been reported to move bidirectionally on actin; all characterized members of the myosin superfamily are specialized for motion towards either the (+)- or (−)-end of the polarized filament. We endeavoured to create new myosin motors that can be signalled to switch their direction of motion, challenging our understanding of mechanical adaptations in unconventional myosins.

In current formulations of the swinging crossbridge model[17], conformational changes are propagated through the catalytic myosin head to drive a rotation of the converter domain. This rotation is amplified by a rigid lever arm extension, generating a directed power stroke toward the (+)-end of the actin filament in most myosin classes. Artificial geometric redirection of the lever arm by insertion of a four-helix bundle generates a (−)-end directed motor[7]. This effect mimics the proposed[18] basis of natural (−)-end directed motion in the specialized myosin VI motor, in which redirection is mediated by a unique insert between the converter domain and lever arm[19]. Structural[12] and functional[8] studies of myosin VI have converged on a refined model in which the unique insert conspires with a converter domain rearrangement[12] to generate a large (−)-end directed stroke. Engineered myosin VI motors[10] with artificial lever arm structures derived from α-actinin[20] showed that 17 residues of the unique insert are sufficient for lever arm redirection, providing a starting point for the designs presented here.

We developed bidirectional transporters over the course of four successive design cycles: (i) minimization of the unique insert of myosin VI to generate a motor with an intermediate lever arm angle; (ii) variation of lever arm length within this altered geometry, leading to length-dependent effects on directionality; (iii) construction of a collapsible lever arm whose effective length is controlled by an external signal; and (iv) assembly of monomeric motor units into processive dimers.

M6CD$_{780}$2R (Fig. 1a) was generated by fusing two spectrin repeats of α-actinin[10,20] following residue 780 of myosin VI, retaining only seven residues of the unique insert. Gliding filament assays (Supplementary Movie S1) show (−)-end directed motion with lower velocities than for M6CD$_{790}$2R (ref. 10), as expected from a predicted lever arm angle that is intermediate between myosin VI and (+)-end directed myosins. M6CD$_{780}$1R was generated by shortening the lever arm of M6CD$_{780}$2R to include only one spectrin repeat. M6CD$_{780}$1R was found to be (+)-end directed (Supplementary Movie S1), implying that the lever arm was truncated beyond the neutral axis of the lever arm rotation (Fig. 1a). In a panel of chimaeric myosins with lever arms fused at five positions between 780 and 790, only fusions in the early portion of the unique insert (at 780 or 783) yielded directionalities that depended on lever arm length (Supplementary Fig. 1).

Dynamically controllable constructs (Fig. 1b) were designed to transition between structures that mimic M6CD$_{780}$1R and M6CD$_{780}$2R. We chose calcium as the signal to control this transition, borrowing a signal that is widely used to control cytoskeletal motors *in vivo*, including distinct mechanisms used to activate skeletal[21] and smooth[22] muscle myosin. Calcium is used as both a natural[23] and engineered[5] regulator of kinesin function, and myosin V is activated by calcium in the *Drosophila* pupil[24].

To achieve dynamic control over lever arm length (Fig. 1b), we incorporated IQ domains derived from the neck region of myosin V (refs 25,26). The helical structure of IQ domains is stabilized by binding to calmodulin. Elevated Ca^{2+} concentration ($[Ca^{2+}]$)can favour dissociation of calmodulin from IQ domains[25,26], which is expected to destabilize the helical structure. Thus, the IQ motif should function as a collapsible element whose effective length can be controlled by $[Ca^{2+}]$. Dissociation of calmodulin causes inhibition of myosin V activity *in vitro*[25], although it is not known whether this regulatory mechanism is used *in vivo*.

We constructed three monomeric myosins with calcium-controlled reversibility (MCaR-2IQ, MCaR-2IQ$_L$ and MCaR-4IQ) by fusing M6CD$_{780}$1R to collapsible lever arm extensions composed of IQ domains (Fig. 1b–d). In gliding filament assays

[1]Department of Bioengineering, Stanford University, Stanford, California 94305, USA, [2]Department of Chemistry, Stanford University, Stanford, California 94305, USA, [3]Department of Structural Biology, Stanford University School of Medicine, Stanford, California 94305, USA. *e-mail: zevry@stanford.edu

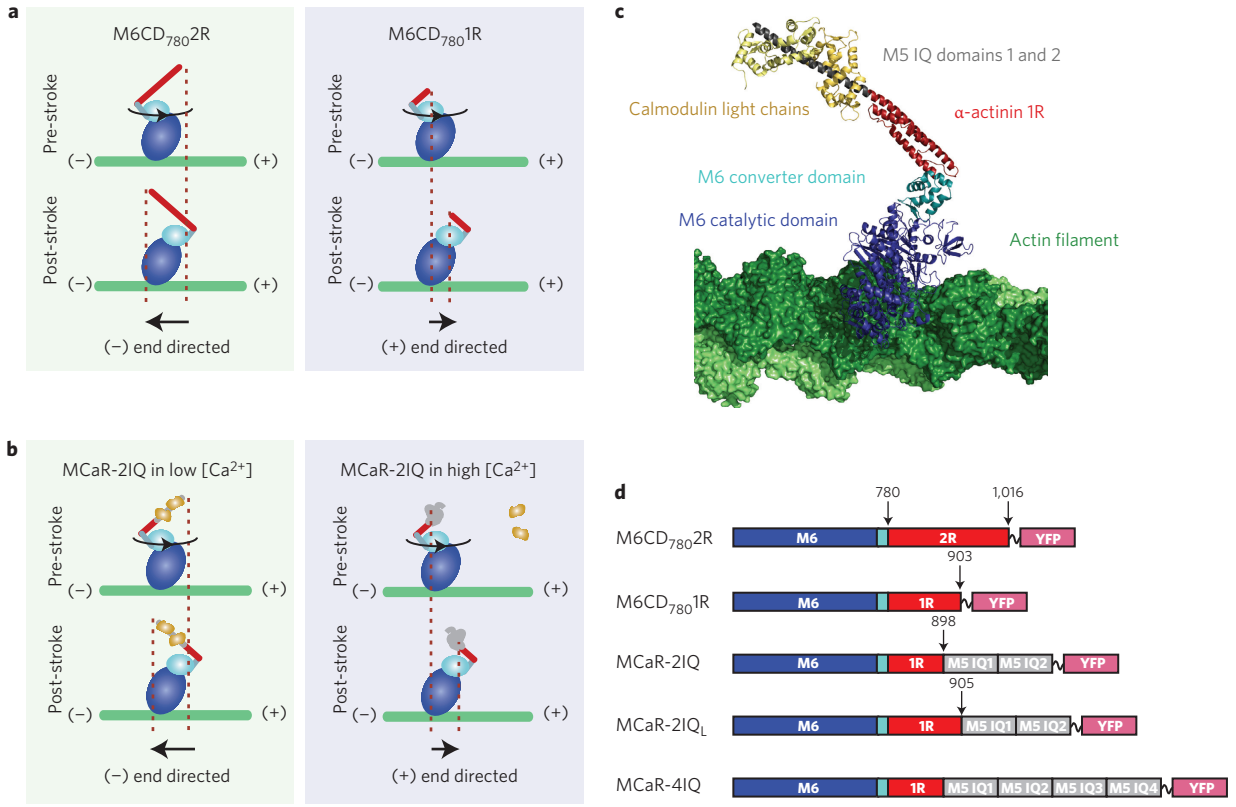

Figure 1 | Engineered myosin designs. An artificial rigid lever arm[20] composed of spectrin-like repeats (red) is fused to myosin VI after residue 780, retaining only seven amino acids of the critical redirecting unique insert. This fusion is predicted to generate an exit angle that is intermediate between myosin VI and (+)-end directed myosins. During the power stroke, rotation of the converter domain (light blue) leads to a net motion of the tip of the lever arm towards the (−)-end of the actin filament for longer lever arms, and towards the (+)-end for shorter lever arms. **a**, Fixed directionality constructs with lever arms composed of differing numbers of spectrin repeats generate motion towards opposite ends of the actin filament. **b**, Calcium-controllable MCaR constructs have chimaeric lever arms composed of a single spectrin repeat fused to two IQ repeats (grey). Under low [Ca^{2+}] conditions, the IQ domains are stabilized by binding to calmodulin (yellow), yielding a long lever arm and (−)-end directed motion. High [Ca^{2+}] favours dissociation of calmodulin, inducing a rigid to flexible transition that shortens the effective lever arm and reverses the direction of motion of the lever arm tip. **c**, Illustration based on crystal structures, showing the expected rigour conformation of MCaR-2IQ bound to the actin filament. **d**, In illustrations and block diagrams, structural modules are represented as follows: blue, myosin VI catalytic domain; light blue, myosin VI converter domain; red, one (1R) or two (2R) spectrin repeats from α-actinin; grey, IQ repeats from myosin V; '∼', $(GSG)_4$ flexible linker; pink, eYFP. Sequences of junctions between modules are shown in Supplementary Fig. 4.

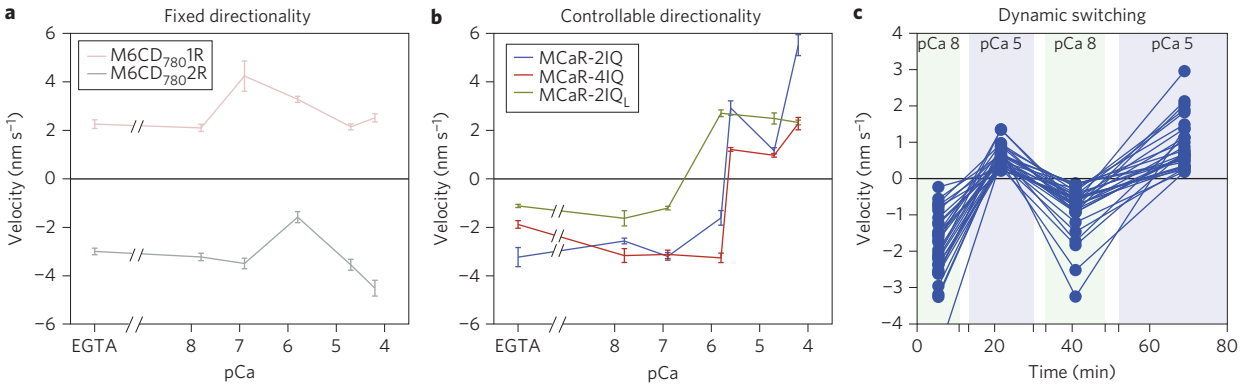

Figure 2 | Gliding filament assays of engineered myosins. Filament velocities were determined in the presence of 2.5 μM calmodulin, 2 mM ATP and the indicated concentrations of free calcium, reported as pCa = $-\log_{10}([Ca^{2+}])$. Positive velocities indicate (+)-end directed motion. Data points with error bars indicate mean ± s.e.m. across sets of filaments (Supplementary Table 1 and Fig. 2). **a**, For fixed directionality constructs, gliding direction is sensitive to engineered lever arm length but not to calcium (Supplementary Movie S1). **b**, MCaR constructs switch directionality near pCa 6, corresponding to approximately micromolar concentrations of free calcium (Supplementary Movies S2–S4). **c**, Velocity time course showing the results of a dynamic switching assay with MCaR-2IQ. pCa buffer was exchanged three times in the flow chamber while observing the same field of filaments (Supplementary Movie S6A,B). Conditions alternated between pCa 8 (10 nM free calcium) and pCa 5 (10 μM free calcium). Of 47 filaments analysed, 30 filaments (shown here) switched directions three times (see Supplementary Fig. 3 for complete tabulation of filament behaviours).

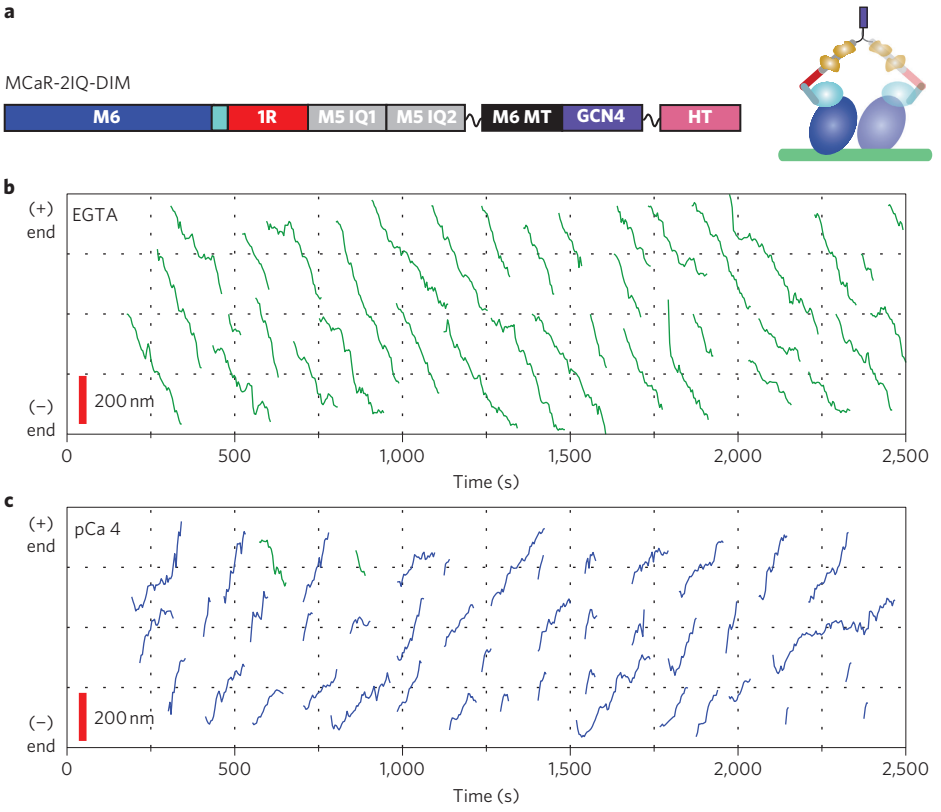

Figure 3 | Processive motility of a dimeric controllable motor. a, Dimers were constructed by fusion of MCaR-2IQ to the medial tail region of myosin VI (black) followed by the GCN4 leucine zipper (green) and a HaloTag (HT, pink). **b**,**c**, Assays of processive motion on immobilized actin filaments were performed in 50 μM ATP, 2 μM calmodulin and EGTA (**b**) or pCa 4 (100 μM free calcium) buffer (**c**). Compiled traces from single fluorophore tracking (Supplementary Movies S7–S9) are shown on a polarized axis representing distance travelled along the actin filament. Directionalities were scored by comparing to subsequent assays of control (−)-end directed M6DI$_{816}$2R-DIM motors[10,11] on the same filaments (Supplementary Movies S8, S9). For MCaR-2IQ-DIM, (−)-end directed traces (green) are ubiquitous in EGTA but represent a small minority (6%) of traces in pCa 4. A total of 75 runs in EGTA and 36 runs in pCa 4 were analysed for velocity and processivity, yielding average velocities of -2.9 ± 1.0 nm s^{-1} in EGTA and $+3.2\pm2.0$ nm s^{-1} in pCa 4, and processive run lengths of 550 ± 50 nm in EGTA and 170 ± 30 nm in pCa 4.

(Supplementary Movies S2–S4), all three MCaR constructs display calcium-sensitive directionality as expected, while the fixed directionality constructs are insensitive to calcium (Fig. 2). We confirmed that gliding filament directionality could be switched by exchanging buffers *in situ* (Supplementary Movies S5,S6), and we tested for dynamic and reversible directionality switching by cycling MCaR-2IQ repeatedly between low and high calcium concentrations (Fig. 2c, Supplementary Movie S6A,B).

Molecular transport carried out by individual motor complexes depends on processive motion along cytoskeletal filaments, such as the hand-over-hand motion observed in dimeric myosin V and myosin VI. We constructed bidirectional dimers (MCaR-2IQ-DIM) by fusing MCaR-2IQ to the medial tail region of myosin VI followed by a leucine zipper (Fig. 3a), as described for previous engineered myosin VI variants[10,11], and asked whether these constructs were capable of processive motion. Many models of processive dimer function emphasize the importance of coordination mediated by intramolecular tension, which may be missing or impaired in MCaR-2IQ-DIM, particularly in the high-[Ca^{2+}] state. However, recent studies of myosin VI constructs with artificial lever arms have found that processive motion may be achieved without optimizing the lever arm geometry or mechanics[10,11]. Together with kinetic modelling[11], these results argue that a high duty ratio may often be sufficient to confer processivity. Using single fluorophore tracking (Supplementary Movies S7–S9), we found that MCaR-2IQ-DIM indeed supports processive motion toward both (−)- and (+)-ends of actin filaments (Fig. 3b,c).

The successful construction of controllable bidirectional motors broadly validates our design based on combining lever arm redirection with dynamic control of lever arm length. However, our results also contain unanticipated details that shed new light on the structure/function relationships in myosin VI and suggest new structural hypotheses to guide future design cycles. Models of the power stroke (Supplementary Section 'Molecular Models') based on alignment to recently reported myosin VI structures[12] do not correctly predict the location of the neutral axis in artificial lever arms fused at residues 780 or 783. The behaviour of these constructs is more successfully predicted by a model that omits the reported converter domain rearrangement[12], and our results suggest that the initial portion of the unique insert through V784 may be required for the rearrangement. In this region of the helical unique insert, residues L777, V780, V784 and N785 form a surface that makes differing contacts in the reported pre-stroke and rigour conformations of the converter[12].

Simple geometric considerations are also insufficient to explain differences in behaviours between the three monomeric MCaR constructs (Fig. 2b). We hypothesize that the low (−)-end directed velocity of MCaR-2IQ$_L$ relative to MCaR-2IQ may result from a decrease in lever arm rigidity due to the insertion of additional residues at the actinin/IQ junction. Accurate prediction of lever arm rigidities will be important for the quantitative design of engineered myosins[13,27]. The local environment of the actinin/IQ junction may also influence the interaction of calmodulin with MCaR-2IQ$_L$, which requires lower calcium concentrations than MCaR-2IQ to

switch to (+)-end directed motility (Fig. 2b). We should note that it is unknown whether calmodulin dissociates from both IQ domains in these constructs. In myosin V, calcium-induced dissociation occurs from IQ2 alone[26], and our most successful structural model for MCaR-2IQ suggests that this could be sufficient for directionality reversal (Supplementary Section 'Molecular Models').

A future challenge will be to optimize the velocities and processivities of controllable bidirectional myosins. MCaR velocities are low in comparison to many natural myosins, which may be explained by the short predicted stroke sizes (Supplementary Section 'Molecular Models') and construct-dependent kinetic perturbations that further extend the long-lived actin-bound phase of the myosin VI cycle, as seen earlier[8]. Velocity improvements may be achieved through alterations of the catalytic domain to accelerate nucleotide turnover, through mutagenesis or replacement of loops that act as kinetic determinants[28], or through construction of chimaeras with faster-moving myosin classes. Higher processivities are also desirable because MCaR-2IQ-DIM is only robustly processive at subsaturating adenosine triphosphate (ATP) concentrations (Fig. 3), and might be achieved through mutagenesis of actin-binding loops[29] or the formation of higher-order complexes.

We have engineered a novel mechanical response to a natural cellular signal. Temporal and spatial modulation of calcium is used to regulate a diversity of cellular processes, and spatially localized changes in calcium levels may be artificially triggered using techniques such as laser-induced photolysis of caged compounds[30]. In a biological context, our designs allow the rewiring of existing signalling mechanisms to control a new output[31], but it would also be desirable to develop motors controlled by orthogonal signals such as small molecules or light[32]. Our conceptual designs based on rigid to flexible transitions are sufficiently general that they should be adaptable to a range of different control signals.

Transitions in lever arm structures such as those described here may be designed to cause changes in a wide range of motor functions controlled by lever arm geometry and mechanics, including step size selection[13] and branchpoint turning[14]. Combined with the optimizations described above, these developments will expand the range of cellular mechanical functions engineered to respond to external signals[31,32] and provide unprecedented levels of control over nanoscale motion in devices that harness the proven capabilities of biological molecular motors[2,3].

Methods

Proteins. DNA constructs were assembled from modules including codons 1–780 (encoding the catalytic domain) and codons 909–992 (encoding the medial tail) of porcine myosin VI, codons 266–502 of *Dictyostelium* α-actinin (truncated earlier when indicated), codons 766–813 (2IQ) or 766–861 (4IQ) of chicken myosin V, eYFP and the GCN4 leucine zipper. Sequences of junctions between structural modules are shown in Supplementary Fig. 4. All constructs were terminated in a C-terminal flag tag (GDYKDDDK), cloned into pBiEx-1 (Novagen), expressed by direct transfection of SF9 cells, and affinity purified as described earlier[8,10,11]. MCaR-2IQ-DIM protein was labelled with TMR-HaloTag ligand (Promega) before elution from anti-flag resin[11].

Buffers for gliding filament assays and single fluorophore tracking. Buffers used for all incubation, wash and assay steps were prepared at the indicated pCa values using 25 mM imidazole-HCl (pH 7.45), 25 mM KCl, 10 mM dithiothreitol (DTT), 2 mM $MgCl_2$, calmodulin as indicated, and Ca-EGTA buffer prepared as described[33] with a total EGTA concentration of 1 mM. Free calcium concentrations were predicted using MaxChelator (http://maxchelator.stanford.edu) and measured using a calcium-sensitive electrode (ThermoScientific). Gliding filament and single fluorophore tracking assays also included ATP as indicated, an ATP regeneration system (1 mM phosphocreatine, 100 μg ml^{-1} creatinephosphokinase), an oxygen scavenging system (0.4% glucose, 0.2 mg mol^{-1} glucose oxidase and 36 μg ml^{-1} catalase) and 1.77 mM trolox as an antibleaching agent.

Gliding filament assays. Dual labelled gliding filament assays were performed as described earlier[8,10] in flow cells coated with mouse monoclonal anti-GFP (Millipore) followed by incubation with myosin-YFP. Videomicroscopy data were collected using simultaneous two-channel imaging of Cy5-actin and TMR-phalloidin on an electron multiplying charge coupled device (EMCCD) camera (Andor) under objective-side total internal reflection fluorescence (TIRF) excitation with a 532 nm diode-pumped solid-state (DPSS) laser (Newport) through a 1.49 NA ×100 objective (Nikon). Filaments were tracked using custom software. Only polarity-marked filaments that travelled further than 100 nm were scored for directionality and velocity.

Single fluorophore tracking. Assays of dimeric myosin were performed as previously described[11] using Alexa 633-phalloidin (Invitrogen) labelled actin filaments attached to the surface via *N*-ethyl maleimide inactivated full-length skeletal muscle myosin (a gift from R. Cooke). Processive runs longer than 100 nm were scored for velocity and run length, and average run lengths were determined after correcting for this minimum threshold and accounting for premature termination events as described earlier[11].

Received 12 September 2011; accepted 19 January 2012; published online 19 February 2012

References

1. Vale, R. D. The molecular motor toolbox for intracellular transport. *Cell* **112,** 467–480 (2003).
2. Korten, T., Mansson, A. & Diez, S. Towards the application of cytoskeletal motor proteins in molecular detection and diagnostic devices. *Curr. Opin. Biotechnol.* **21,** 477–488 (2010).
3. Goel, A. & Vogel, V. Harnessing biological motors to engineer systems for nanoscale transport and assembly. *Nature Nanotech.* **3,** 465–475 (2008).
4. Liu, H. *et al.* Control of a biomolecular motor-powered nanodevice with an engineered chemical switch. *Nature Mater.* **1,** 173–177 (2002).
5. Konishi, K., Uyeda, T. Q. & Kubo, T. Genetic engineering of a Ca^{2+} dependent chemical switch into the linear biomotor kinesin. *FEBS Lett.* **580,** 3589–3594 (2006).
6. Nomura, A., Uyeda, T. Q. P., Yumoto, N. & Tatsu, Y. Photo-control of kinesin-microtubule motility using caged peptides derived from the kinesin C-terminus domain. *Chem. Commun.* 3588–3590 (2006).
7. Tsiavaliaris, G., Fujita-Becker, S. & Manstein, D. J. Molecular engineering of a backwards-moving myosin motor. *Nature* **427,** 558–561 (2004).
8. Bryant, Z., Altman, D. & Spudich, J. A. The power stroke of myosin VI and the basis of reverse directionality. *Proc. Natl Acad. Sci. USA* **104,** 772–777 (2007).
9. Park, H. *et al.* The unique insert at the end of the myosin VI motor is the sole determinant of directionality. *Proc. Natl Acad. Sci. USA* **104,** 778–783 (2007).
10. Liao, J-C., Elting, M. W., Delp, S. L., Spudich, J. A. & Bryant, Z. Engineered myosin VI motors reveal minimal structural determinants of directionality and processivity. *J. Mol. Biol.* **392,** 862–867 (2009).
11. Elting, M. W., Bryant, Z., Liao, J-C. & Spudich, J. A. Detailed tuning of structure and intramolecular communication are dispensable for processive motion of myosin VI. *Biophys. J.* **100,** 430–439 (2011).
12. Menetrey, J., Llinas, P., Mukherjea, M., Sweeney, H. L. & Houdusse, A. The structural basis for the large powerstroke of myosin VI. *Cell* **131,** 300–308 (2007).
13. Vilfan, A. Elastic lever-arm model for myosin V. *Biophys. J.* **88,** 3792–3805 (2005).
14. Vilfan, A. Myosin V passing over Arp2/3 junctions: branching ratio calculated from the elastic lever arm model. *Biophys. J.* **94,** 3405–3412 (2008).
15. Lee, L. K., Ginsburg, M. A., Crovace, C., Donohoe, M. & Stock, D. Structure of the torque ring of the flagellar motor and the molecular basis for rotational switching. *Nature* **466,** 996–1000 (2010).
16. Roostalu, J. *et al.* Directional switching of the kinesin Cin8 through motor coupling. *Science* **332,** 94–99 (2011).
17. Holmes, K. C., Schröder, R. R., Sweeney, H. L. & Houdusse, A. The structure of the rigor complex and its implications for the power stroke. *Phil. Trans. R. Soc. Lond. B* **359,** 1819–1828 (2004).
18. Wells, A. L. *et al.* Myosin VI is an actin-based motor that moves backwards. *Nature* **401,** 505–508 (1999).
19. Menetrey, J. *et al.* The structure of the myosin VI motor reveals the mechanism of directionality reversal. *Nature* **435,** 779–785 (2005).
20. Anson, M., Geeves, M. A., Kurzawa, S. E. & Manstein, D. J. Myosin motors with artificial lever arms. *EMBO J.* **15,** 6069–6074 (1996).
21. Gordon, A. M., Homsher, E. & Regnier, M. Regulation of contraction in striated muscle. *Physiol. Rev.* **80,** 853–924 (2000).
22. Somlyo, A. P. & Somlyo, A. V. Signal transduction and regulation in smooth muscle. *Nature* **372,** 231–236 (1994).
23. Wang, X. & Schwarz, T. L. The mechanism of Ca^{2+}-dependent regulation of kinesin-mediated mitochondrial motility. *Cell* **136,** 163–174 (2009).
24. Satoh, A. K., Li, B. X., Xia, H. & Ready, D. F. Calcium-activated Myosin V closes the Drosophila pupil. *Curr. Biol.* **18,** 951–955 (2008).
25. Krementsov, D. N., Krementsova, E. B. & Trybus, K. M. Myosin V: regulation by calcium, calmodulin, and the tail domain. *J. Cell Biol.* **164,** 877–886 (2004).

26. Trybus, K. M. *et al*. Effect of calcium on calmodulin bound to the IQ motifs of myosin V. *J. Biol. Chem.* **282,** 23316–23325 (2007).
27. Parker, D., Bryant, Z. & Delp, S. L. Coarse-grained structural modeling of molecular motors using multibody dynamics. *Cell. Mol. Bioeng.* **2,** 366–374 (2009).
28. Sweeney, H. L. *et al*. Kinetic tuning of myosin via a flexible loop adjacent to the nucleotide binding pocket. *J. Biol. Chem.* **273,** 6262–6270 (1998).
29. Krementsova, E. B., Hodges, A. R., Lu, H. & Trybus, K. M. Processivity of chimeric class V myosins. *J. Biol. Chem.* **281,** 6079–6086 (2006).
30. Zheng, J. Q. & Poo, M. M. Calcium signaling in neuronal motility. *Annu. Rev. Cell Dev. Biol.* **23,** 375–404 (2007).
31. Yeh, B. J., Rutigliano, R. J., Deb, A., Bar-Sagi, D. & Lim, W. A. Rewiring cellular morphology pathways with synthetic guanine nucleotide exchange factors. *Nature* **447,** 596–600 (2007).
32. Levskaya, A., Weiner, O. D., Lim, W. A. & Voigt, C. A. Spatiotemporal control of cell signalling using a light-switchable protein interaction. *Nature* **461,** 997–1001 (2009).
33. Tsien, R. & Pozzan, T. Measurement of cytosolic free Ca^{2+} with quin2. *Meth. Enzymol.* **172,** 230–262 (1989).

Acknowledgements

The authors thank M.W. Elting for valuable discussions and assistance, R. Cooke for providing full-length muscle myosin, and S. Sutton for providing purified actin. This work was supported by a Pew Scholars Award (to Z.B.), the NIH (grant no. DP2 OD004690 to Z.B.), an NSF Graduate Research Fellowship (to L.C.), an AHA Predoctoral Fellowship (to M.N.) and a Stanford Graduate Fellowship (to T.D.S.).

Author contributions

L.C., M.N. and Z.B. designed the molecular motor constructs. L.C., M.N. and T.D.S. performed experiments on fixed directionality motors. L.C. and M.N. performed experiments on bidirectional motors. L.C. analysed the experimental data. D.P., L.C. and M.N. performed structural modelling. Z.B. conceived and supervised the project. L.C. and Z.B. wrote the paper. All authors discussed the results and commented on the manuscript.

Additional information

The authors declare no competing financial interests. Supplementary information accompanies this paper at www.nature.com/naturenanotechnology. Reprints and permission information is available online at http://www.nature.com/reprints. Correspondence and requests for materials should be addressed to Z.B.